

Self-Affine Fractal Interfaces from Immiscible Displacement in Porous Media

M. A. Rubio,^(1,2) C. A. Edwards,⁽¹⁾ A. Dougherty,⁽¹⁾ and J. P. Gollub^(1,3)

⁽¹⁾*Department of Physics, Haverford College, Haverford, Pennsylvania 19041*

⁽²⁾*Departamento de Física Fundamental, Universidad Nacional de Educación a Distancia, Apartado Correos 60141, Madrid 28080, Spain*

⁽³⁾*Department of Physics, University of Pennsylvania, Philadelphia, Pennsylvania 19104*

(Received 5 June 1989)

Wetting immiscible displacement of one fluid by another in a porous medium yields self-affine (anisotropic) fractal interfaces between the two fluids. Water-air interfaces are characterized experimentally by a scale-dependent roughness $w(L) = AL^\beta$, with $\beta = 0.73 \pm 0.03$, independent of the capillary number Ca , and $A \propto Ca^{-0.47 \pm 0.06}$. The exponent β is related to the "box" and "divider" dimensions by $D_b = 2 - \beta$ and $D_d = 1/\beta$, respectively.

PACS numbers: 47.55.Mh, 68.45.Gd

The displacement of one fluid by another in a porous medium displays a rich variety of behavior,¹ depending on the properties of the two fluids, including their viscosities and effectiveness in wetting the medium.² This problem has been of fundamental interest in part because fractal interfaces form under certain conditions. For example, when the displacing fluid is less viscous and less effective in wetting the medium, the invaded region is filamentary and has scaling properties described by diffusion-limited aggregation (DLA) with a fractal dimension $D = 1.71$ (for two-dimensional geometries).³ Slow displacement by a nonwetting fluid, on the other hand, is understood in terms of "invasion percolation" models^{2,4} with $D = 1.82$. Some other situations do not lead to fractal interfaces at all.⁵

The fractal interfaces previously studied are statistically self-similar^{6,7} when magnified equally in all directions. In this paper, we describe a geometrical study of the interfaces formed when the displacing fluid is more viscous and more effectively wets the medium. The invaded region is then continuous, but random local pinning by capillary forces leads to a rough interface that is well described as a self-affine⁸ (that is, anisotropic) fractal. In that case, various methods of computing D give different results, and the most useful exponent is one that describes the scaling of the width of the interface with measurement scale.

If the displacing fluid preferentially wets the medium, as in our experiments, the fluid moves through the smaller pores at lower pressures than those required to move through the larger ones. This leads to certain preferred locations for the interface, so there can be many stable states. Microscopic examples of such random pinning phenomena are fairly common in condensed matter systems; for example, in charge-density wave motion in conductors.⁹ The nonlinear response of such a fluid system to an applied force was carefully studied by Stokes, Kushnick, and Robbins,¹⁰ though the geometry of the interface could not be investigated in that work.

Two theoretical approaches to the problem of wetting

immiscible displacement¹¹ are available in the literature: a stochastic partial differential equation for the motion of an interface in a random medium,¹² and a microscopic model that considers various mechanisms for advancing individual segments of the interface.¹³ In both approaches the interface may be either in constant motion or "pinned," depending on the noise amplitude in Ref. 12, or the contact angle in Ref. 13. However, no results from either model concerning the fractal properties of the moving interfaces have been published, although Cieplak and Robbins¹³ suggested that the interface might be a self-affine (anisotropic) fractal.

Our experiments were performed in a thin horizontal cell of dimensions 55 cm in the direction of motion (y), 17 cm in the transverse (x) direction, and 0.15 cm deep. The top and bottom plates were glass, separated by a Teflon gasket. The porous medium consisted of tightly packed glass beads that were ultrasonically cleaned, thoroughly rinsed with distilled water, and dried in an oven. We applied a similar procedure to the glass plates. We used three different bead sizes b , with average diameters of 100, 200, and 350 μm , and a diameter variation δ of about $\pm 20\%$.

Water containing a small amount of dye to improve contrast was injected into the cavity at one end of the cell. A constant flow velocity was obtained by means of a syringe driven by a high-precision stepper motor. This system allowed us to control the pumping velocity with nominal resolution better than 1% for the slowest velocities used. After the interface spreads from the injection point across the whole width of the cell, a constant average velocity of the interface can be defined. Our analysis only includes the patterns obtained after this spreading occurred.

The motion of the interface was recorded with a charge-coupled-device videocamera, and digitized with a spatial resolution of 512×480 pixels and 8-bit intensity resolution. The imaging system was arranged to capture only the central 10 cm of the interface in the x direction, to avoid edge effects. Thus the pixel size is 180 μm .

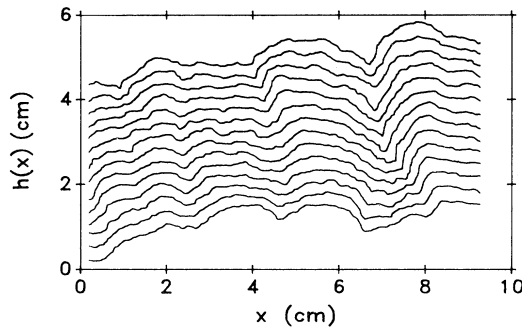


FIG. 1. Plot of fourteen successive interfaces at $Ca = 4.93 \times 10^{-3}$. The time interval between single interfaces is 30 s.

The relevant control parameter is the modified capillary number, defined as $Ca = U\mu b^2/k\gamma$, where U is the average velocity of the interface, μ is the dynamic viscosity of water, γ is the air-water interfacial tension, b is the bead size, and k is the permeability. The capillary number measures the ratio of the viscous pressure ($U\mu b/k$) to the capillary pressure (γ/b) on the scale of the pore size. The ratio b^2/k is approximately 5.1×10^3 for this system. We varied Ca between roughly 10^{-3} and 10^{-1} ; therefore the viscous pressure drop in the water is always smaller than the capillary pressure drop across the interface.

For the cavity and the bead sizes used, we have an average of four to fifteen interconnected bead layers in the vertical direction, and therefore three-dimensional effects could be significant. The interface is in fact slightly fuzzy due to differential interface advancement at different heights, but in practice this fuzziness is less than about 0.5 mm, or about $\frac{1}{3}$ of the depth. Therefore representing these interfaces as lines $h(x)$ is a good approximation down to this scale. We processed the images as described in Ref. 14 to determine the interfacial shape $h(x)$.

A typical sequence of interfaces at $Ca = 4.93 \times 10^{-3}$ is shown in Fig. 1, with a time interval of 30 s between images. The roughness of the interface on a range of scales is evident. The apparent roughness of the interface increases with decreasing Ca . We also note that the interfaces usually do not present overhangs; i.e., the functions $h(x)$ are single valued, reflecting the low probability of air trapping. The interface advances by coherent jumps involving several pores.

How should such rough interfaces be characterized? In studies of interfacial phase transitions¹⁵ and surface growth models,¹⁶ interfacial irregularity is often characterized by the roughness or width $w(L)$, which is defined as the rms value of the fluctuations of $h(x)$ over a length scale L . More explicitly, $w(L) = \langle \langle [h(x) - \langle h \rangle_L]^2 \rangle \rangle^{1/2}$, where $\langle h \rangle_L$ is the average height over a segment of horizontal length L , and the double brackets stand for averaging over all the segments of length L that may be defined in the x direction. Application of this concept to

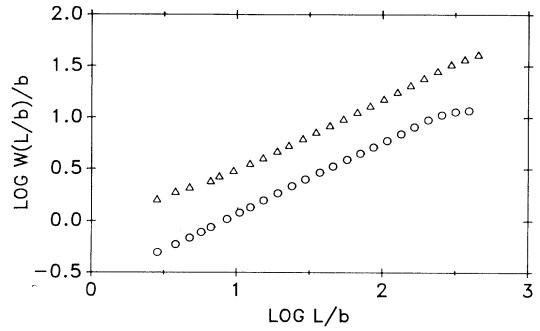


FIG. 2. Plot of roughness vs length scale at two different values of Ca for bead size $b = 200 \mu\text{m}$. $Ca = 2.47 \times 10^{-3}$ (Δ) and 9.78×10^{-3} (\circ).

the interfaces of the present experiments is straightforward. Figure 2 shows a log-log plot of $w(L)$ for two different values of Ca , where all lengths are expressed in units of the bead size $b = 200 \mu\text{m}$. Each plot represents the average of $w(L)$ from thirty different images obtained in the same run. We find power-law behavior, $w(L) = AL^\beta$, extending over slightly more than one decade. At small length scales, the measurements are limited by the slight three dimensionality of the interfaces, and ultimately by the bead size. At the largest length scales, and for sufficiently high Ca , $w(L)$ begins to saturate.

Similar scaling behavior with the same exponent is found over the entire range of Ca and bead sizes studied. In Fig. 3 we show β as a function of $\log_{10}(Ca)$ for three different bead sizes. Within the experimental uncertainty, β is independent of both Ca and b , yielding an average value $\beta = 0.73 \pm 0.03$, where the quoted uncertainty is the standard deviation. Figure 4 shows the dependence of A on Ca on a log-log scale. Although there is significant scatter, the points collapse fairly well onto a single line $A \propto (Ca)^\alpha$; linear regression yields $\alpha = -0.47 \pm 0.06$.

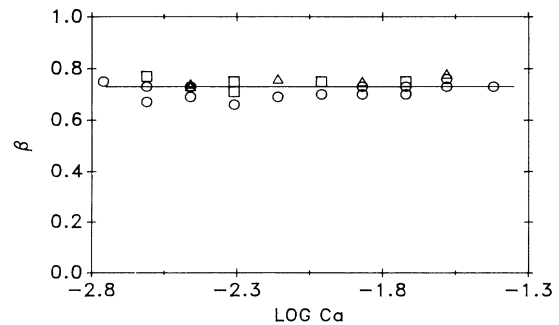


FIG. 3. Roughness exponent vs Ca for $b = 100$ (\square), 200 (\circ), and $350 \mu\text{m}$ (Δ). The uncertainties are comparable to the size of the symbols. The line corresponds to the average value of $\beta = 0.73 \pm 0.03$.

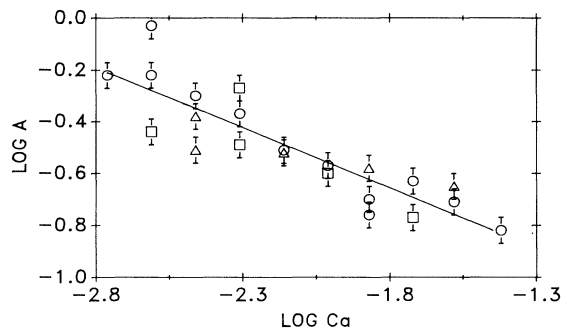


FIG. 4. Roughness amplitude vs Ca for $b=100$ (\square), 200 (\circ), and 350 μm (\triangle). The line is a least-squares fit by $A=A_0Ca^\alpha$, which yields $\alpha=-0.47\pm 0.06$.

The fact that β differs from unity implies that fluctuations in the interface shape scale differently in the x and y directions and that the interfaces are therefore self-affine fractals.^{6,7} Mandelbrot has thoroughly discussed the problem of the dimensionality of self-affine structure⁸ and has shown that several different dimensions may be computed, although they must be interpreted carefully. The “box” dimension, D_b , is computed by counting the number $N(L)$ of boxes of size L needed to cover the curve, with $N(L) \propto L^{-D_b}$. The “divider” dimension, D_d , is obtained by walking a divider of length L along the curve and measuring the length of the curve $\Lambda(L)$ in units of L ; then $\Lambda(L) \propto L^{-D_d}$. These quantities are related to β as follows: $D_b=2-\beta$, and $D_d=1/\beta$. The two dimensions are different when $\beta \neq 1$.

We have carried out direct measurements of D_b and D_d . In computing the latter, it is necessary^{8,17} to magnify the scale in the y direction until the exponent D_d reaches a constant value. We find experimentally that $D_b=1.18\pm 0.08$ and $D_d=1.36\pm 0.08$, whereas the predicted values based on the measured β are $D_b=1.27\pm 0.03$ and $D_d=1.37\pm 0.05$, respectively, where the reported uncertainties are again the standard deviations. The results obtained are consistent with the predicted expressions.¹⁸ This strengthens the conclusion that these interfaces are well described as self-affine fractals, with scaling properties that are independent of capillary number and bead size, though the amplitude A , in units of the bead size, varies approximately as $Ca^{-1/2}$. Furthermore, the roughness exponent may be measured more precisely than the other quantities and has a more intuitive physical interpretation.

The constancy of the roughness exponent β seems remarkable, and suggests that efforts to explain the observation $\beta=0.73\pm 0.03$ may be worthwhile. Preliminary numerical results¹⁹ for the interfaces in the discrete model of Ref. 13 yield scaling behavior with $0.70 < \beta < 0.74$, consistent with our observations. Another type of growth model, a stochastic and nonlinear generalization of the diffusion equation for the propagation of an

interface, has been studied by renormalization-group methods.²⁰ Though its applicability to the present experiments is not completely clear, it does produce self-affine interfaces with roughness exponents between 0.5 and 1, depending on the properties of the noise.

The fact that A decreases with Ca implies that the effects of the pore scale randomness become less significant at higher flow velocities. However, the physical mechanism leading to the particular dependence on $Ca^{-1/2}$ remains an open question. Some insight into the existence of an upper bound on $w(L)$ can be obtained by balancing the viscous pressure drop ($\mu U w/k$) over a region of length w against the maximum capillary pressure difference that might arise due to dispersion in the bead size ($\delta\gamma/b^2$, where δ is the estimated bead-size dispersion). The maximum possible value for $w(L)$ is then expected to be $w_{\text{max}}=\delta/Ca$. For $Ca=3.82\times 10^{-2}$, $b=200$ μm , and $\delta\sim 80$ μm , we have $w_{\text{max}}/b\sim 10$. This limit is consistent with the saturation in $w(L)$ observed at the highest Ca , but is generally larger than $w(L)$, and has a different dependence on Ca than the observed amplitude A .

We acknowledge useful discussions with D. A. Kessler, H. Levine, M. O. Robbins, J. P. Stokes, and D. A. Weitz. These experiments evolved from the collaboration of Ref. 5. Our work was supported by National Science Foundation (Low Temperature Physics Program) Grant No. DMR-85-03543. We also appreciate computing equipment provided by the U.S. Department of Defense University Research Initiative Program under Contract No. DARPA/ONR-N00014-85-K-0759 to Princeton University. M.A.R. acknowledges partial support from a fellowship of the NATO Scientific Committee.

¹For a recent review, see G. M. Homsy, *Annu. Rev. Fluid Mech.* **19**, 271 (1987).

²R. Lenormand, E. Touboul, and C. Zarcone, *J. Fluid Mech.* **187**, 165 (1988).

³J. D. Chen and D. Wilkinson, *Phys. Rev. Lett.* **55**, 1892 (1985); K. J. Maloy, J. Feder, and T. Jossang, *Phys. Rev. Lett.* **55**, 2688 (1985); K. J. Maloy, F. P. Boger, J. Feder, T. Jossang, and P. Meakin, *Phys. Rev. A* **36**, 318 (1987).

⁴R. Chandler, J. Koplik, K. Lerman, and J. Willemsen, *J. Fluid Mech.* **119**, 249 (1982); D. Wilkinson and J. Willemsen, *J. Phys. A* **16**, 3365 (1983); D. Wilkinson and M. Barsony, *J. Phys. A* **17**, L129 (1984); R. Lenormand and C. Zarcone, *Phys. Rev. Lett.* **54**, 2226 (1985).

⁵J. P. Stokes, D. A. Weitz, J. P. Gollub, A. Dougherty, M. O. Robbins, P. M. Chaikin, and H. M. Lindsay, *Phys. Rev. Lett.* **57**, 1718 (1986).

⁶B. B. Mandelbrot, *The Fractal Geometry of Nature* (Freeman, New York, 1982).

⁷J. Feder, *Fractals* (Plenum, New York, 1988).

⁸B. B. Mandelbrot, *Phys. Scr.* **32**, 257 (1985); B. B. Mandelbrot, in *Fractals in Physics*, edited by L. Pietronero and E. Tossati (Elsevier, Amsterdam, 1986), pp. 3–28.

⁹D. S. Fisher, *Phys. Rev. B* **31**, 1396 (1985).

¹⁰J. P. Stokes, A. P. Kushnick, and M. O. Robbins, *Phys. Rev. Lett.* **60**, 1386 (1988).

¹¹Good wetting implies that all pores are accessible to the invading fluid and the invasion percolation model is inapplicable.

¹²J. Koplik and H. Levine, *Phys. Rev. B* **32**, 280 (1985).

¹³M. Cieplak and M. O. Robbins, *Phys. Rev. Lett.* **60**, 2042 (1988).

¹⁴A. Dougherty and J. P. Gollub, *Phys. Rev. A* **38**, 3043 (1988).

¹⁵M. E. Fisher, *J. Chem. Soc. Faraday Trans. 2* **82**, 1569 (1986).

¹⁶F. Family, *J. Phys. A* **19**, L441 (1986).

¹⁷S. R. Brown, *Geophys. Res. Lett.* **14**, 11 (1987); **14**, 1095 (1987).

¹⁸The accuracy of such computations has been discussed by B. Dubuc, J. F. Quiniou, C. Roques-Carmes, C. Tricot, and S. W. Zucker, *Phys. Rev. A* **39**, 1500 (1989). These authors also find that numerically measured box dimensions tend to be lower than expected.

¹⁹M. O. Robbins (private communication).

²⁰E. Medina, T. Hwa, M. Kardar, and Y.-C. Zhang, *Phys. Rev. A* **39**, 3053 (1989).